Pushing the Boundaries of Modular-Integrated Construction: A Symmetric Skeleton Grammar-Based Multi-objective Optimization of Passive Design for Energy Savings and Daylight Autonomy

Qianyun Zhou[1], Fan Xue[2]*

This is the peer-reviewed post-print version of the paper:

Zhou, Q., & Xue, F. (2023). Pushing the boundaries of modular-integrated construction: A symmetric skeleton grammar-based multi-objective optimization of passive design for energy savings and daylight autonomy. *Energy and Buildings*, 296, 113417. Doi: 10.1016/j.enbuild.2023.113417

The final version of this paper is available at: https://doi.org/10.1016/j.enbuild.2023.113417.
The use of this file must follow the Creative Commons Attribution Non-Commercial No Derivatives License, as required by Elsevier's policy.

Highlights

- Automatic MiC envelopes and layout generation by a novel SSG-MOO method.
- Multi-objective optimization formulation for passive MiC design.
- A pilot MiC study in Hong Kong produced 5 selected Pareto optima out of 625.
- Up to 0.42% energy savings and 9.71% spatial daylight autonomy improvement against the baseline.
- A multi-level analysis of results and design strategies for practitioners.

Abstract

Modular-integrated Construction (MiC) is an emerging construction technique promoted in the building sector for high productivity and low waste emission in the construction phase; yet, the standardized modules also bring new challenges, such as balancing passive energy efficiency and spatial daylight autonomy, to the operational phase. This paper proposes a Symmetric Skeleton Grammar-based Multi-Objective Optimization (SSG-MOO) method to formulate parametric MiC envelopes and detailed layout, with the two objective functions being energy efficiency and interior daylight performance in the operational phase. Pareto optima of the SSG-MOO, computed by the Non-dominated Sorting Genetic Algorithm II, are generally verified and analyzed in three levels, i.e., MOO's solution space, SSG layout, and MiC design parameters. A case study of MiC residential building in Hong Kong demonstrated the SSG-MOO method through five new passive MiC designs (i.e., spatial reorganization of three architectural modules, and parameter tuning of the envelops and corridors), achieving up to 0.42% energy savings and 9.71% spatial daylight autonomy improvement compared to the baseline design. The contribution of this paper is two-fold, including a novel and sound SSG-

[1] Qianyun Zhou, MArch,
Research Assistant, Department of Real Estate and Construction, The university of Hong Kong, Pokfulam, Hong Kong, China
E-mail: qianyunz@hku.hk ORCiD: https://orcid.org/0000-0002-5466-6225

[2] Fan Xue, PhD
Assistant Professor, Department of Real Estate and Construction, The university of Hong Kong, Pokfulam, Hong Kong, China
E-mail: xuef@hku.hk ORCiD: https://orcid.org/0000-0003-2217-3693
* Corresponding author, Tel: +852 3917 4174, Fax: +852 2559 9457, Email: xuef@hku.hk

MOO formulation for parametric MiC designs, and offering time-efficient and evidence-based design tactics for MiC designers and industrial practitioners to push boundaries of MiC.

Keywords

Modular-integrated Construction; Multi-objective Optimization; Symmetric Skeleton Grammar; Energy Efficiency; Daylight Performance; Passive Generative Design

1 Introduction

Worldwide, over 34% of final energy is consumed by the building and construction sector, emitting a third of green gas emissions (UNEP 2022). As a high-rise high-density city, Hong Kong receives roughly 60% of greenhouse gas emissions from the building sector, and the energy consumption has risen by 13.7% from 2010 to 66416 TJ in 2020 in the residential sector (EMSD 2022). The high energy consumption necessitates the development of novel sustainable construction technologies. Recently, a list of innovative sustainable construction technologies, such as modular construction and 3D printing, offer more advantages of enhancing productivity, reusability, and occupational safety than energy savings over the construction life cycle (Wang et al. 2020; Li et al. 2022).

Modular-integrated Construction (MiC) is a novel construction technology best-known in the construction phase. MiC assembles free-standing integrated and volumetric modules before on-site installation (Pan & Hon 2020). According to Abdelmageed & Zayed (2020), MiC outperforms many construction technologies, including prefabrication, panelized construction, and hybrid construction, with higher productivity and safety, maintaining lower energy consumption and wastage in the construction phase. MiC also facilitates manufacturing, assembly, supply chain, and logistics management (Li et al. 2022). Therefore, MiC is highly promoted in Hong Kong, where around 20,000 new units of public housing projects are expected to use MiC technology for the 10-year period from 2022/23 to 2031/32 (HKHA 2022). However, the standard modularization also brings new challenges, such as constrained building designs and exponential combinations of modules.

However, few studies have addressed optimum MiC designs in the operational phase, which involves up to 80%–90% of the total energy consumption (Habash 2022). Echenagucia et al. (2015) demonstrated that the optimal design of buildings could successfully improve indoor environmental comfort. Appropriate natural illumination and thermal comfort, for example, can save energy from lighting, cooling, and heating throughout the operational phase. Furthermore, MiC is a new technology without detailed written standards. Therefore, it is urgent and vital to study the optimal design for energy-efficient MiC buildings for the operational phase.

Generally, energy-efficient MiC building designs are highly related to passive design strategies, such as proper building layouts, windows, and insulation materials in the walls and roof (Baños et al. 2011; Fang & Cho 2019). Building layouts, different from other architectural components (such as windows), are infeasible to reconstruct by variables only, due to the topological properties. Some state-of-the-art research has suggested the connection patterns between multiple modules, but the lack of a generic rule has made widespread implementation challenging. Previous studies suggested shape grammar as a transferable formulation for automatic layout generation in computer-aided design systems, which was operated through replacement rules on finite shapes (Haakonsen et al. 2023). Over the past fifty years, shape grammar has evolved to encode the design language of classic architectural projects and has been applied to generalize design guidelines to represent and generate a diverse range of architectural layouts. However, the existing shape grammars are subject to specific building types and require to be redefined manually in each design situation. Applying traditional shape grammars to guide the replacement rules thus is a labor-intensive procedure. Additionally, MiC layouts exhibit symmetry and standardization, notably in high-density Hong Kong. Thus, a generic and symmetric generation grammar is required for efficiently creating MiC layouts. In addition to energy efficiency, there are additional objectives such as visual comfort and health (Echenagucia et al. 2015). In the literature, multi-objective optimization (MOO) is often adopted to guide designers in generating optimal passive design with complex objectives (Hamdy et al. 2016).

This paper proposes a symmetric skeleton grammar-based Multi-objective Optimization (SSG-MOO), a computer-aided passive design method, for energy-efficient MiC designs. First, a symmetric skeleton grammar is defined to formulate the layout and envelope of a standard MiC story using a set of design variables, including window-to-wall ratios, window heights, corridor axis, corridor lengths, and module distribution. Two objective formulations are then defined, with numerical simulations of energy use intensity (*EUI*) and spatial daylight autonomy (*sDA*), for evaluating the building performance of MiC design. MOO algorithms can optimize the SSG formulation against the two objectives by perturbating the passive MiC designs, with two hard constraints on the total modules and total floor area. In-depth analysis of the Pareto front are presented for validation and insights, with comparisons between the SSG-MOO's optima and the baseline design. A pioneering 19-story MiC housing project was studied in Hong Kong to demonstrate the proposed method. The contribution of this paper is thus twofold: (i) A novel SSG-MOO formulation of energy-efficient and ambient-daylighting MiC designs and (ii) a time-efficient method and evidence-based design principles for planners and designers to push the boundaries of MiC.

The remainder of the paper is structured as follows: Section 2 reviews previous research for building layout grammars and passive design optimization. Section 3 elaborately presents the research method in four parts and proposes an SSG-MOO method, emphasizing the symmetric skeleton grammar, for energy-efficient MiC designs. Then, Section 4 explains the experimental settings and analyzes the results in three levels. Finally, Sections 5 and 6 discuss the main findings and summarize the conclusions.

2 Literature review

2.1 Modular building design rules and grammars

In prefabricated and modular construction, layout rules and grammars have been studied with prefabricated modules. Gan et al. (2019) parameterized the modular building layouts by measuring one core area and multiple wings; each wing consisted of a corridor and adjacent household modules. Gan (2022) later extended the parameterized modular layouts with a graph model representing the topological, geometric, and semantic information. Zhang et al. (2021) then explored the connection patterns of multiple-shaped architectural modules to generate layout rules. Nevertheless, for MiC typologies, which are highly efficient and standardized, a systematic and scalable grammar for generating standard floor layouts is still lacking.

Shape grammar has been developed as a systematic formalization of recursive rules to represent and generate floor layouts of various building types since the 1970s in the literature, as illustrated in Figure 1 (Stiny & Gips 1972; Ning & Peiman 2018; Haakonsen et al. 2023). For example, Stiny and Mitchell (1978) employed a parametric shape grammar to generate the ground plans of Palladio's villas. Koning and Eizenberg (1981) encoded the design language of Frank Lloyd Wright's prairie house with a shape grammar derivation. Similarly, Gülen (1996) and Duarte (2005) created varied architectural layouts for different types of residential houses by defining the connection rules of the shape grammar. Ruiz-Montiel et al. (2013) studied proximity relationships of architectural spaces with given design requirements using shape grammars and reinforcement learning, presenting diverse design solutions for single-family housing. Moreover, Paulino et al. (2023) developed the *Reviver* shape grammar for converting historic buildings into social housing; the *Reviver* grammar helped to generate various types of housing layouts, i.e., studios, one-bedroom, and two-bedroom apartments.

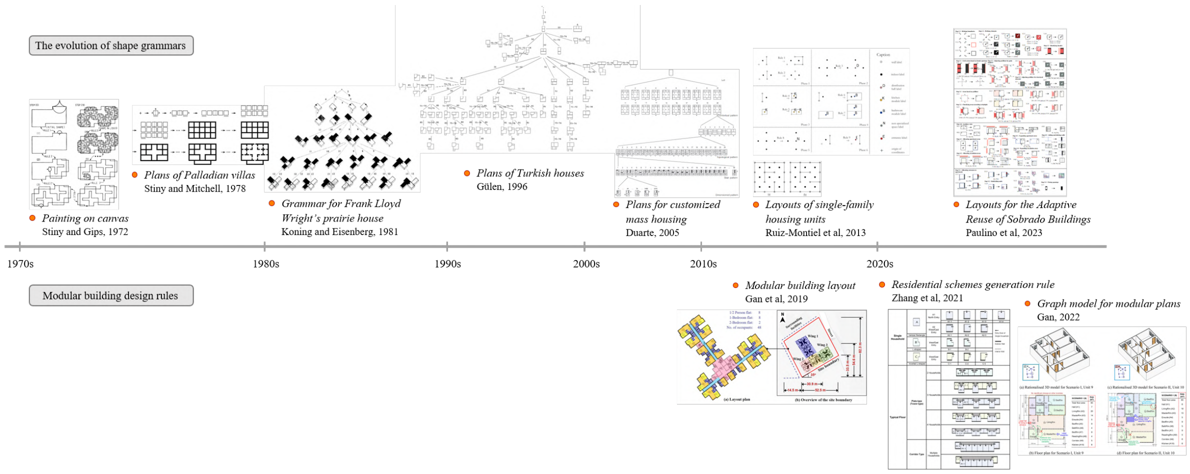

Figure 1. The timeline review of shape grammars and modular building design rules in the literature

The benefits of shape grammar include encoding the topological variations and presenting universal properties for building layouts by summarizing the architectural design guidelines. However, the existing shape grammars often need to be manually redefined by designers regarding different built objects; and the generated building footprints are commonly non-standardized. MiC with mass construction and standardized manufacturing properties cannot be fully adapted to existing shape grammars. Thus, a concise and scalable generative grammar is urgently needed for the represent the standardized modules of MiC.

2.2 Multi-objective optimization for passive building design

Passive building design promotes solutions with comfortable indoor environments that effectively reduce energy consumption during the operational phase (Sadineni et al. 2011). Later, computer-aided passive design optimization relieved designers from manually modifying numerous architectural parameters (Stevanović 2013). The optimization is often an iterative procedure coupled with numerical simulation tools. The popular tools for building performance simulation in optimization studies are *EnergyPlus* and *TRNSYS* (Nguyen et al. 2014). Usually, designers are required to address multiple – and sometimes conflictive – objectives simultaneously for achieving a comfortable indoor environment, such as proper illumination and thermal comfort (Liu et al. 2020; Zheng et al. 2023). Therefore, the MOO method has been widely adopted to find the optimal solutions for comfortable and low-energy passive building design (Clarke & Hensen 2015; Hamdy et al. 2016).

Existing MOO techniques can be classified into two categories: aggregate weight functions and Pareto-based optimization methods (Baños et al. 2011). Aggregating functions transform all the objectives into a single weighted-sum function to optimize the objectives. However, aggregating functions have several limitations, such as constant weights and linear summation, that oversimplify complex objectives and return only a single solution after the lengthy search process (Hajela & Lin 1992). In contrast, Pareto-based MOO examines a set of trade-off optimal solutions (a Pareto set) between each objective and determines appropriate solutions (Nguyen et al. 2014). Pareto-based MOO can overcome the major drawbacks of aggregating functions. The common algorithms for Pareto-based MOO are metaheuristics, including Genetic Algorithm (GA), Covariance Matrix Adaptation Evolutionary Strategy (CMA-ES), Harmony Search (HS), Particle Swarm Optimization (PSO), and Ant Colony Optimization (ACO). GA, in particular the Non-dominated Sorting Genetic Algorithm (NSGA-II) (Hamdy et al. 2016), was the most prominent Pareto-based MMO algorithm for building performance problems in the literature (Evins 2013; Ascione et al. 2017; Ciardiello et al. 2020). Popular optimization environments for NSGA-II include *Matlab* (Ljung & Singh 2012), *modeFRONTIER* (Clarich et al. 2011), and *Grasshopper* (*Wallacei*, *Galapagos*, *Octopus*) on *Rhinoceros* (Makki et al. 2015).

Existing MOO studies of passive designs using NSGA-II in the literature were primarily conducted from three perspectives, i.e., the building envelopes, floor layout, and building form-finding. For example, with NSGA-II, Didier et al. (2013) studied the optimal thermophysical properties of the dwelling's envelope in two French climates, targeting reduced annual energy consumption and improved summer comfort. Echenagucia et al. (2015) further explored the optimal envelope variables to minimize energy consumption for heating, cooling, and lighting in four urban contexts (i.e., Palermo, Torino, Frankfurt, and Oslo). The research was conducted on an office building by optimizing the number, position, shape, and type of windows and the thickness of masonry walls. Moreover, the study developed by Zhang et al. (2021) showed the effectiveness of optimizing floor layouts to enhance energy efficiency in the early design stage for a residence case in Beijing. Based on four different climate zones, an MOO study by Konis et al. (2016) concluded that the optimum building form and orientation could considerably improve the performance of daylighting and energy efficiency.

Therefore, it can be concluded that passive design optimization based on MOO can effectively achieve energy reductions in heating, ventilation, air conditioning (HVAC) and artificial lighting by modifying architectural properties (Tian et al. 2018). This paper thus aims to design energy-efficient and daylight-autonomous MiC that rely the least on heating, cooling, and lighting, using an MiC design grammar and optimum modular fenestration and layouts.

3 Research methods

This paper presents a bi-objective passive design optimization method focusing on MiC envelope and layout. As shown in Figure 2, the method contains four parts: (1) A symmetric skeleton grammar of combinatorial MiC design variables; (2) Definition of the SSG-MOO problem of energy-efficient and ambient-daylighting MiC with constrains; (3) MiC design generation by solving SSG-MOO; (4) Pareto optima selection and multi-level verification and analysis.

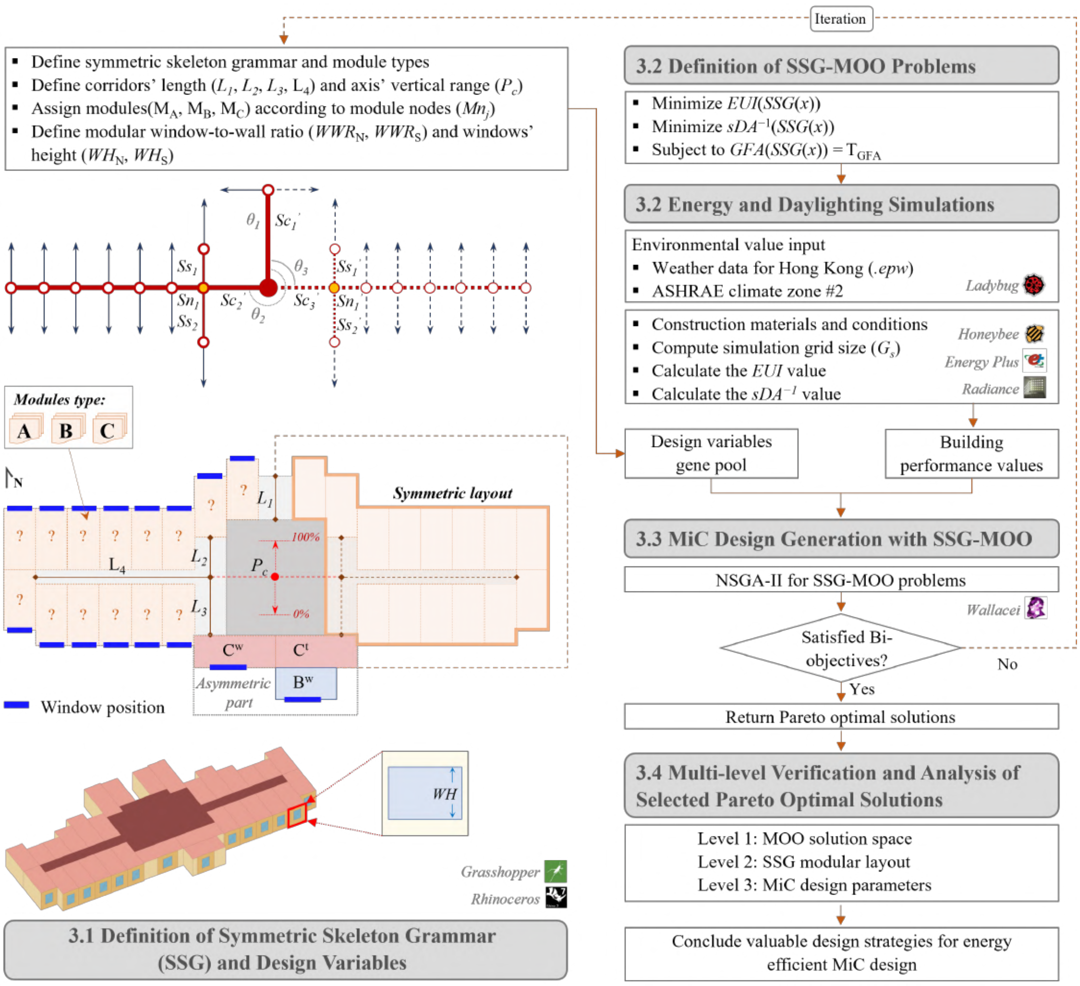

Figure 2. The proposed SSG-MMO method for energy-efficient and ambient-daylighting MiC design.

3.1 Definition of symmetric skeleton grammar and design variables

This section defines a symmetric skeleton grammar deriving from the basic features of shape grammar and aesthetics to represent the spatial topology between MiC modules. The grammar first indicates the core point from which the axis of symmetry is subsequently defined. Later, the skeletons of the main corridors (Sc_i) are defined, where i denotes the number of circulation corridors. By rotating Sc_i through the angle θ (clockwise rotation from Y-axis), the spatial topology of the corridor skeletons to the core point is obtained, which is saved as Sc_i'. The grammar constructs sub-skeletons for sub-corridors (Ss_i) and locations for modules by determining the placement of sub-skeleton nodes (Sn_j) or module nodes (Mn_j). Then, the modules are arranged by vectors (Mv_j). Here j represents the total number of modules in relation to the number of occupants. The entire layout is horizontally symmetrical. Therefore, for symmetrical wings, the computed decision is only required once to generate the mirrored wing; this setting can considerably increase the computational speed. The derivation tree diagram for this grammar is illustrated in Figure 3. The grammar well represents the majority layouts of new residential buildings in Hong Kong; for example, Figure 4 shows the standard layouts for public housing in Hong Kong (HKHA 2020).

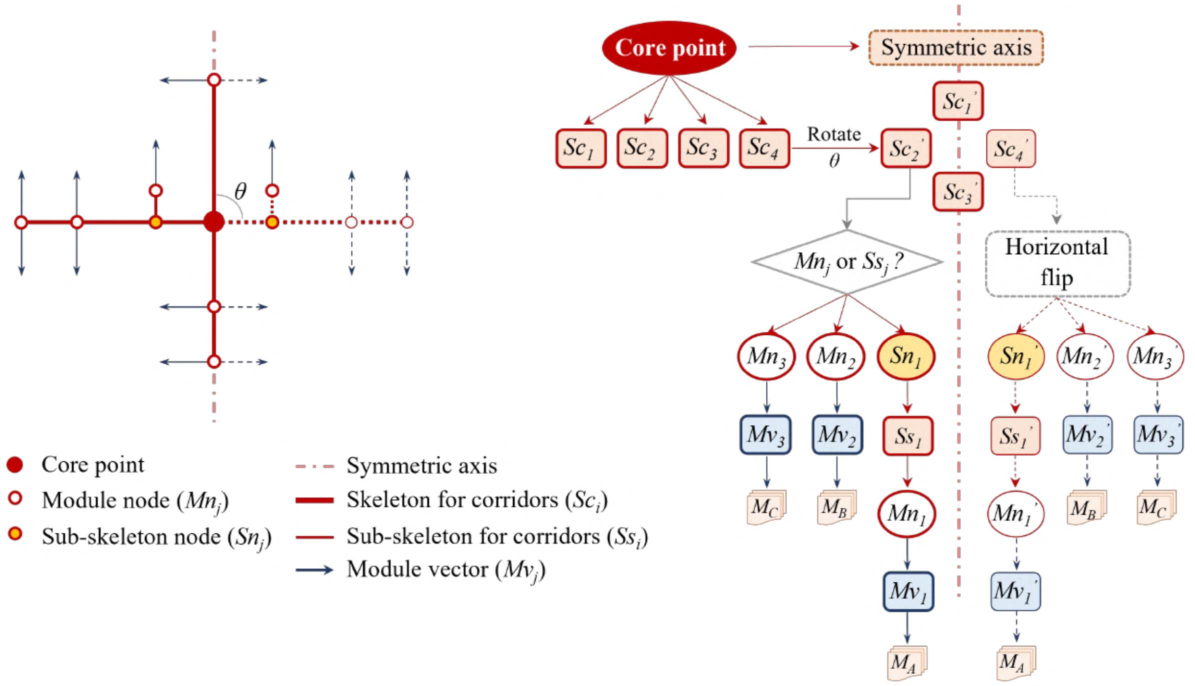

Figure 3. The derivation tree diagram for the proposed symmetric skeleton grammar.

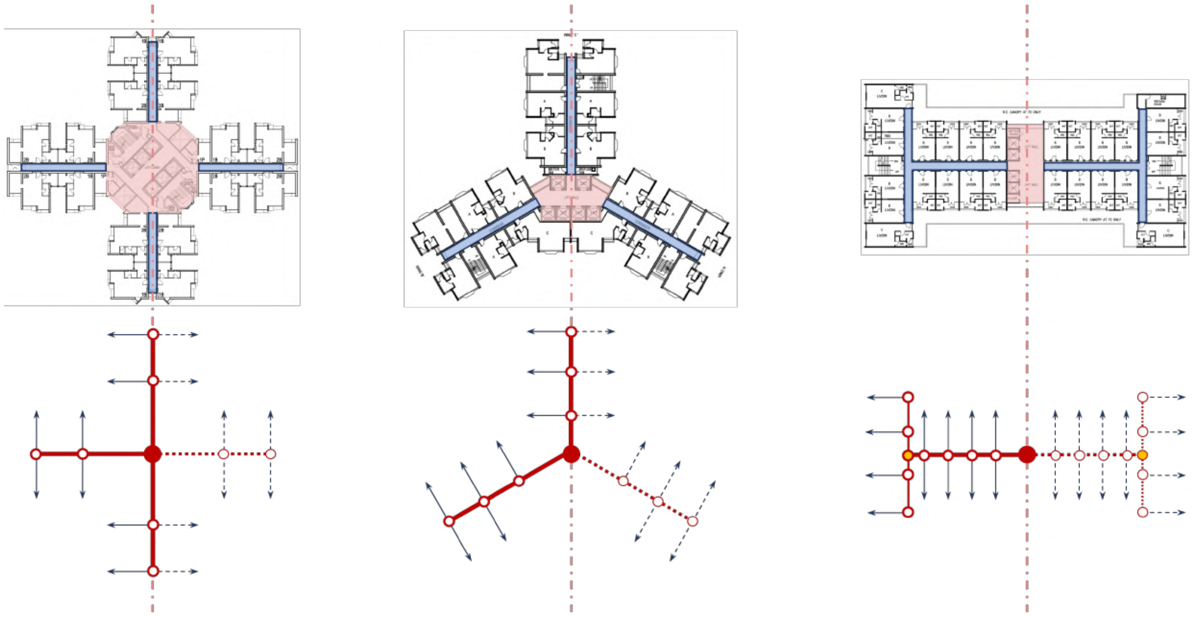

Figure 4. Examples of symmetric skeleton grammar representation of public housing layouts in Hong Kong.

With the symmetric skeleton grammar, a MiC model can be decoded and parameterized in *Rhinoceros3D (Ver.7.0)* with *Grasshopper*. The former is the professional 3D CAD software with high compatibility, whereas the latter is a graphical algorithm editor interacting 3D modeling with numerical simulations (McNeel 2023). As shown in Figure 2, a MiC layout consists of symmetric and asymmetric parts. The symmetric parts include three main corridors (Sc_1', Sc_2', Sc_3') with two nodes (Sn_1, Sn_1') generating sub-corridors (Ss_1, Ss_2, Ss_1', Ss_2'), where θ_1, θ_2, and θ_3 are 0°, 270°, and 90°, respectively. The midpoint of the corridor axis (Sc_2', Sc_3') can be altered within the vertical range (P_c). Three parameters of corridors' lengths (L_1, L_2, L_3) are variable, while L_4 is a constant value when the number of modules per floor is determined. Different modules (e.g., M_A, M_B, M_C) are arrangeable for the layout according to Mv_j, while each module has a parametric window with the *WWR* and height variables on the north (WWR_N, WH_N) or south (WWR_S, WH_S) side of the module. The asymmetric part is usually much smaller than the symmetric ones in size, which differs between projects. The three fixed-location modules (C^w, C^t, B^w) are arranged in the bottom of the south, also with parametric windows.

3.2 Definition of SSG-MOO problem of energy-efficient and ambient-daylighting MiC

We formulate the MOO of passive MiC envelope and layout design as a bi-objective problem:

$$\begin{aligned} &\textbf{arg min}_{x\in X} \;\; EUI(SSG(x)),\, sDA^{-1}(SSG(x)) \\ &\textbf{subject to} \;\; GFA(SSG(x)) = \mathrm{T_{GFA}}, \\ &\qquad\qquad\quad \Sigma\, Mn_j = \text{Constant} \end{aligned} \tag{1}$$

Where *SSG* maps input design parameters to an MiC layout, *EUI* is the energy use intensity (kWh/(m^2·yr)) that is calculated by dividing the total energy used per year by the gross floor area (Konis et al. 2016), sDA^{-1} refers to the inversed spatial daylight autonomy (to minimize) that expresses the annual deficiency of ambient daylight levels for the interior environment, quantifying the percentage of minimum received brightness during daytime working hours in the target space (Heschong et al. 2012), the first constraint is that the *SSG*'s gross floor area is equal to the expected value (T_{GFA}), x stands for a combination of the n design variables (x_1, x_2, ..., x_n), and X means the set of all possible combinations. And the second constraint is the constant number of total modules.

The *EUI* computation is based on an integrated energy model of multi-feature data, including local climate data, construction materials, construction type, and HVAC. The energy model (*.osm*) can be translated into the *.idf* file via the *OpenStudio* component in *Honeybee (Ver.1.5)* and run on the built-in *EnergyPlus* program (Roudsari & Pak 2013). The target meteorological data can be downloaded from the *EnergyPlus* weather website through the *Ladybug (Ver.1.5) EPWmap* component (ASHRAE 2021). As a result, the *EUI* and related end-use value (i.e., heating, cooling, interior lighting, and the other end-uses) can be calculated.

The sDA^{-1} is the reciprocal of *sDA*. In general, *sDA* assesses whether the floor area receives a minimum target illuminance of 300lx for at least 50% of the year during standard occupied hours ($sDA_{300/50\%}$) on the horizontal work plane. According to the LEED V4.1 standard (standard for green building design, construction, operations, and performance), the average $sDA_{300/50\%}$ value for the regularly occupied floor area should be reached 40% to earn one point of standard daylight evaluation, and 50% for two points (Pilechiha et al. 2020; USGBC 2022). The formula for *sDA* can be defined as (Pilechiha et al. 2020): $sDA = \Sigma_{\rho=1\ldots N} ST(\rho) / N$, where $ST(\rho) = 1$ if $st_\rho \geqslant \tau t_y$, and $ST(\rho) = 0$ if $st_\rho \leqslant \tau t_y$. st_ρ is the occurrence count above the *sDA* illuminance threshold at point ρ; t_y is the annual timestamp count, and τ denotes the temporal fraction threshold. Assuming an N-point grid with function $ST(\rho)$, the value turns to one when point ρ in the grid has a minimum required illuminance that exceeds a given percentage of the total occupied time, and zero vice versa. Later, the *Honeybee-Radiance* components launch the annual daylight simulation for each sensor based on the preset grid size (G_s). Since *sDA* takes probability between zero and one, the interval of sDA^{-1} is one to ∞. By minimizing the sDA^{-1}, the SSG-MMO in Eq. (1) tends to improve MiC layouts toward less deficiency of ambient daylighting.

3.3 MiC design generation with SSG-MOO

Many MOO algorithms can solve the SSG-MOO problem in Eq. (1). For simplicity and clarity, the NSGA-II algorithm implemented in *Wallacei (Ver. 2.7)*, an add-on that interacts with simulation data with *Honeybee* and *Ladybug* in *Grasshopper* (Makki et al. 2018), is adopted in the remainder of this paper. The design variables described in Section 3.1 are transferred as genes, while *EUI* and sDA^{-1} values in Eq. (1) are then positioned and sorted among the objective space. The major algorithmic parameters of NSGA-II are population size and crossover/mutation index.

The output of NSGA-II is the Pareto optima that is the set of non-dominated solutions. A dominated solution indicates all its objective values are inferior than another (or more) solutions (Deb et al. 2002; Li et al. 2023). However, it can be time-consuming and computationally challenging for decision-makers to analyze the entire Pareto optima or quickly select a unique ‘best solution’. Proper selection, verification, and analysis are thus essential for prioritizing the most promising solutions for MiC practitioners.

3.4 Multi-level verification and analysis of selected Pareto front

This paper employs verification and analysis in three levels for validating the selected solutions on the Pareto front. The three levels are MOO solution space, SSG modular layout, and MiC design parameters.

Firstly, the bi-objective ranking of the Pareto optimal solutions is sorted, compared, and analyzed. The overall density and trending curves of Pareto front are summarized for the alternative. Then, we extend the ‘Utopia’ point method with the baseline MiC layout as the second reference solution in the solution space. The ‘Utopia’ point is the virtual position of the ideal solution in the objective space, obtained by minimizing each objective function without regard for other objective function (Showkatbakhsh & Makki 2022). A rectangular-shaded area can be drawn between the ‘Utopia’ point and the baseline MiC reference point. Pareto optimal solutions in the rectangular are most desirable for decision-makers, due to all the objectives are superior than the baseline. This screening approach can effectively save time and effort for practitioners to select multiple Pareto optimal solution(s) while keeping the variation and diversity of the selected subsets.

Secondly, the modular layouts of the selected Pareto optima are generated by SSG for visualization and assessment. The selection and arrangement of multiple modules can be assessed and compared together with the baseline MiC layout. The layouts’ improvement effects on the target performance are analyzable accordingly.

Finally, passive design variables are explored, and general design trends for energy-efficient MiC design are presented. The data sample is based on the selected Pareto optimal solutions. This paper applies Spearman’s correlation to testing the correlations between the two optimization objectives and the eleven design variables. The Spearman’s correlation coefficient (r) is a value between −1 and 1. And the significant (e.g., $p < 0.001$) correlations often indicate interesting relations to investigate and interpret further with domain knowledge.

4 Experimental tests

4.1 Experimental settings

A pioneering 19-story MiC residential building was the test case in this paper. The building is a university student hostel located at 142 Pokfulam Road, Hong Kong, Latitude 22°15’51.76” N, Longitude 114°8’7.72” E, and to be completed by the second quarter of 2024 (HKSAR 2021). Figure 5 (a) depicts the climatic indicators for the building, explicitly showing the mean-minimum-maximum dry bulb temperature and global horizontal radiation values for each month. As shown in Figure 5 (a), the dry-bulb temperatures reach more than 30 °C in summer in Hong Kong, with average winter levels around 10 °C; and the summer lasts approximately six months. Figure 5 (b) shows the baseline MiC layout, which was designed by a professional architect consultant, consisting of a core tube with six different types of modules. Modules B^w,

C^w, and C^t remain spatially constant in this study, and the corresponding window features were added to the optimization calculation. The spatial layouts for the three modules, M_A, M_B, and M_C, were then reorganized in the optimization. The width and height of each module type are fixed at 2.5 m and 3.15 m, respectively. Those modules differ primarily in terms of length and windows' features.

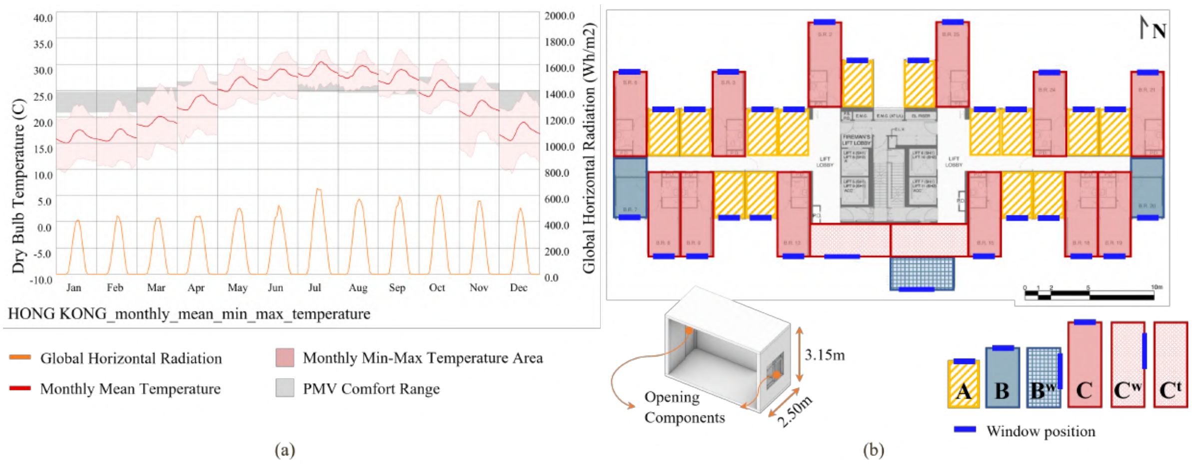

Figure 5. (a) Annual climate indicators for Hong Kong SAR. (b) The baseline MiC layout.

Table 1 lists the design variables considered in the SSG-MOO experiments, along with data units and ranges. The design variables were divided into two types: corridors and windows. L_1 was based on $Sc_1{}'$, varied from 0 to 2 m, and controlled the corridor length on the north; L_2 and L_3, which were based on Ss_1 and Ss_2, respectively, modified the length of the northern and southern sub-corridors, with values ranging from 1m to 6m. P_c guided the vertical movement (0% to 100%) of the horizontal corridors along the axis of symmetry. WWR_N and WWR_S varied between 20% and 70% for the south and north facades, respectively. Moreover, WH_N and WH_S were optimized in the range of 1.0m to 2.5m. The T_{GFA} in this experiment was 531.34 m^2, and the modules number (C) was 31. To fulfill the requirement for the number of occupants on each floor, modular amount and L_4 were fixed values of 31 and 13.75 m, respectively.

Table 1. Independent variables in MiC parametric design excluding selection of modules.

Type	Component	Unit	Variable's value range
Corridor	Corridor length (L_1, L_2, L_3)	m	$0 \leqslant L_1 \leqslant 2.00$; $1.00 \leqslant L_2, L_3 \leqslant 6.00$
	Vertical range for the corridor axis (P_c)	%	$0 \leqslant P_c \leqslant 100$
Window	Window-to-Wall Ratio (WWR_N, WWR_S)	%	$20 \leqslant WWR_N, WWR_S \leqslant 70$
	Window height (WH_N, WH_S)	m	$1.0 \leqslant WH_N, WH_S \leqslant 2.5$

Table 2 lists the material settings for MiC envelopes. In this case, the single clear glass had a thickness of 0.006m, where the U-value was 5.78 W/m^{2}K, the Solar Heat Gain Coefficient (SHGC) value was 0.775, and the visible transmittance value was 0.881. The wall and floor slab thicknesses were set as 0.14 m and 0.1 m, respectively, with U-values as 3.72 W/m^{2}K and 2.89 W/m^{2}K. The above parameters referred to the energy modeling recommendations for residential buildings specified in the Hong Kong environmental evaluation (Qin & Pan 2020). According to *Honeybee* Heat Cool Templates, the HVAC system was configured as a "*Window AC with baseboard electric*" for high-rise apartments. In addition, the construction set applied "*ASHRAE 90.1 2019*" for building vintages and "*2-Hot*" for the climate zone. The numerical simulations were then conducted with a resolution grid size (G_s = 0.5m).

Table 2. Material parameter settings for MiC envelopes.

Envelopes	Thickness (m)	k (W/mK)	U_ Factor (W/m^{2}K)	SHGC	Visible Transmittance
Single clear glass	0.006	0.900	5.78	0.775	0.881
Wall	0.140	2.160	3.72	–	–
Floor	0.100	2.160	2.89	–	–

For the NSGA-II algorithm settings, both the generation size and generation count were chosen as 25, producing a total population of 625. And the index for crossover and mutation distribution was set as 20 in *Wallacei*. The rest parameters of NSGA-II algorithm were set according to the existing literature expertise (Chantrelle et al. 2011; Makki et al. 2015; Showkatbakhsh & Makki 2022).

4.2 Experimental results and analysis

The experiments were conducted on a desktop computer with an Intel (R) Core i7-10700 CPU @ 2.90 GHz processor and 32 GB memory. The total time cost was 15.56 hours to solve the SSG-MOO problem by the NSGA-II algorithm and the simulations. A total of 39 Pareto optima were returned. Within the Pareto-Utopia shaded area, as shown in Figure 6 (a), the five selected MiC Pareto optima decreased the *EUI* values and increased daylight performance for the same floor area and units as the baseline case. The visualization analysis of daylight and energy end-use for each of these five options is shown in Figures 6(b) and (c). In Figure 6(b), the closer the color is to red, the more daylight can be received, and the closer it is to blue, the less. In particular, the energy end use (in heating, cooling, lighting, equipment, and water) of these five options is presented in detail in Figure 6(c).

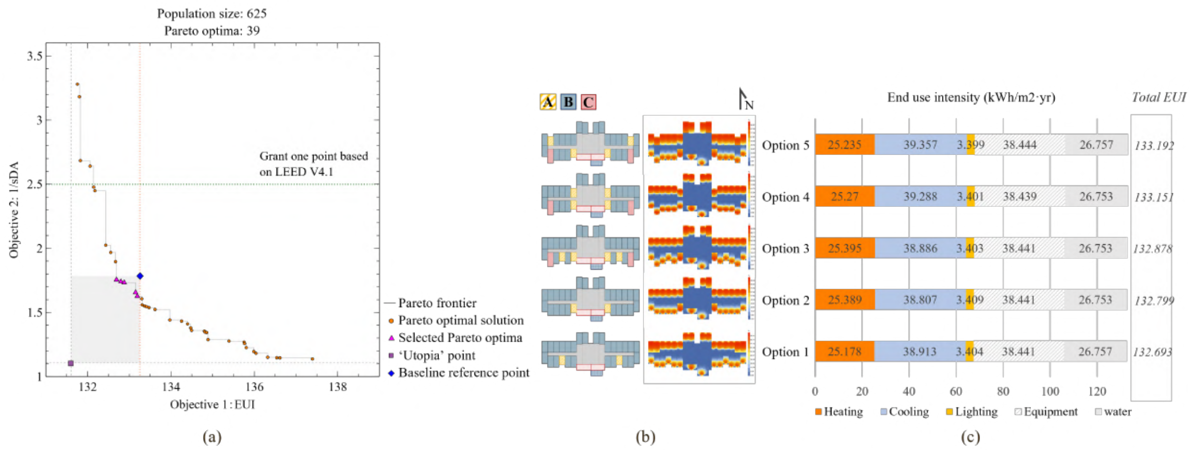

Figure 6. The selection and comparative analysis of the five MiC Pareto optima. (a) 39 Pareto optima solution space; (b) Modular layouts of the five selected MiC Pareto optima with daylighting visualization; (c) End use intensity of the selected.

4.2.1 On the MOO solution space level

Every dot in Figure 6 indicates a Pareto optimum, i.e., a Pareto optimal solution, and they depict the Pareto front collectively. In Figure 6 (a), the purple square symbol represents the 'Utopia' point, the blue diamond symbol shows the location of the baseline MiC scheme, and the magenta triangular symbol highlights the five selected MiC Pareto optima. The closer a point is to the square "Utopia" point, the superior the behavior of the specific solution in relation to that objective. The rectangular shading area bounded by the 'Utopia' point and the baseline case suggests the most promising Pareto optimal solutions, which were superior than both objective values – or dominate over – the input baseline case.

In addition to the five options located in the Pareto-Utopia shaded area, Figure 6(a) shows five more Pareto optimal solutions between the baseline point and the horizontal dash line $sDA^{-1} = 2.5$. The threshold $sDA^{-1} = 2.5$ (or $sDA = 40\%$) will grant at least one point based on LEED V4.1 standard. These five options might also be available for the project team to consider, if they would like to emphasize on the *EUI*. In the remainder of this section, we mainly focus on the five MiC designs in Figure 6 (b) without loss of generality.

4.2.2 On SSG modular layout level

Figure 6(b), (c) and Table 3 comprehensively compare the layouts of the five selected MiC Pareto solutions and the baseline project concerning the improvement magnitude in energy and daylighting performance. In Table 3, the improvement magnitude [% Imp.*] is the percentage increase or decrease, where v_0 is the EUI value of the baseline scheme, and v_1 is the *EUI* value of the calculated option; w_0 represents baseline scheme's sDA, and w_1 represents the *sDA* value of the calculated option. For the MOO process, modules B^w, C^w, and C^t (three modules arranged horizontally below) remain spatially constant in this paper. The baseline MiC design solution consists of 12 M_A, 2 M_B, and 14 M_C. And the baseline scheme simulated the EUI as 133.259 kWh/m^2·yr and the sDA as 56.05%.

Option 1 reduces annual energy consumption by 0.42% per square meter compared to the baseline scheme. In terms of modular layout, Option 1 arranges more M_B than the baseline one and tends to be essentially flat at the northern boundary. Similarly, Options 2 and 3 are close to the horizontal line in the layout of the modules on the north side. Option 2 has a higher energy efficiency than Option 3, with close indoor daylighting performance. Option 4, which arranges the three modules evenly on the north and south sides, computed the EUI as 133.151 kWh/m^2·yr, a reduction of 0.08% compared to the baseline one, while the sDA improves by 7.78%. Option 5 significantly improves the performance of daylighting with an increase of 9.71%, while its building energy consumption is reduced by only 0.05%. It can also be noticed that from Option 1 to Option 5, as the value of sDA increases from 57% to 61.49%, the energy consumption of cooling increases from 38.913 kWh/m^2·yr to 39.357 kWh/m^2·yr, while the energy use of lighting gradually decreases.

Table 3. Objective values and improvements of the five Pareto optimal solutions of MiC designs in Figure 6 (b).

Option	*EUI* (kWh/m²·yr)	*EUI* [% Imp.*]	*sDA* (%)	*sDA* [% Imp.*]
1	132.693	0.42	57.00	1.69
2	132.799	0.35	57.47	2.53
3	132.878	0.29	57.71	2.96
4	133.151	0.08	60.41	7.78
5	133.192	0.05	61.49	9.71
Baseline	133.259	-	56.05	-

*: Improvement by percentage, $(v_0 - v_1)/v_0 \times 100\%$ for *EUI*, $(w_1 - w_0)/w_0 \times 100\%$ for *sDA*.

Overall, from Option 1 to Option 5, the annual energy consumption per square meter of the MiC designs gradually increases, while the daylight performance shows an opposite trend. Compared with the baseline scheme, the five Pareto optimal schemes all meet the requirements of the LEED V4.1 standard to obtain two points for daylight assessment, and all have improved the energy efficiency for MiC design.

4.2.3 On MiC design parameters level

Figure 7 shows the Spearman's rank correlations between the design variables and the two objectives. Figure 7 contains histograms at diagonal subfigures, and the lower half involves scatter plots and trend lines, where the color and size of the circle in the upper triangle indicate the sign and value of the correlation coefficient (r). Note that six insignificant variables (P_c, L_1, L_2, L_3, WH_N, WH_S) in this case are hidden in Figure 7. Specifically, the findings reveal significant and very strong correlations ($r = \pm 0.91$, $p \leqslant 0.001$, $N = 39$) between WWR_S and the two objectives.

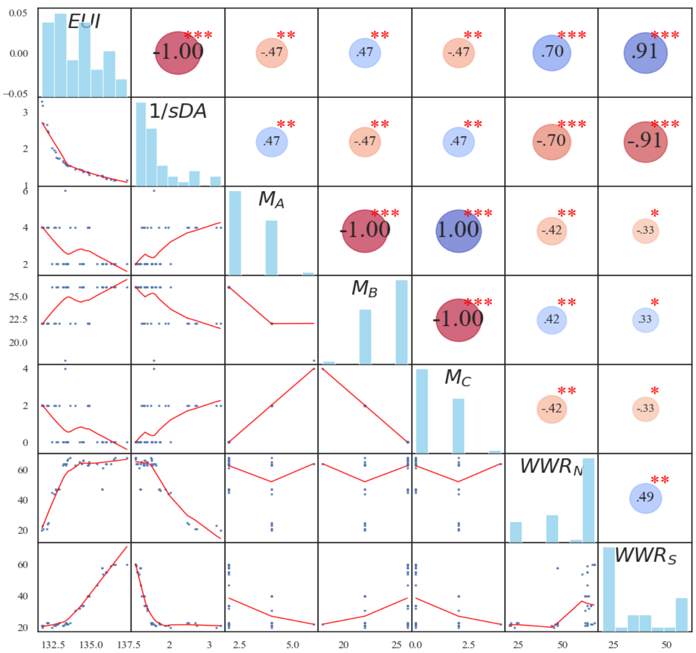

Figure 7. Results of Spearman's correlation analysis based on 39 Pareto optima, with histograms, scatter plots, and the correlation coefficient r (cool color indicates positive, size stands for strength) and significance ($^{***}p \leqslant 0.001$, $^{**}p \leqslant 0.01$, $^{*}p \leqslant 0.05$, two-tailed).

Similarly, WWR_N shows strong correlations ($r = \pm 0.70$, $p \leqslant 0.001$, $N = 39$) with EUI and sDA^{-1}. For the three types of modules, the number of M_B has a moderate positive correlation ($r = 0.47$, $p \leqslant 0.01$, $N = 39$) with EUI, whereas the number of M_A and M_C has a moderate negative correlation ($r = -0.47$) with EUI. It can be found an opposite result in correlation coefficients of M_B and M_A, M_C calculated by sDA^{-1}. Moreover, the results show that the number of M_B has a robust negative correlation with the number of M_A and M_C, with a coefficient of –1.0 ($p \leqslant 0.001$), while the number of M_A has a robust positive correlation (1.0) with the number of M_C. However, the values of WH_N and WH_S did not show significant correlations with EUI or sDA^{-1}.

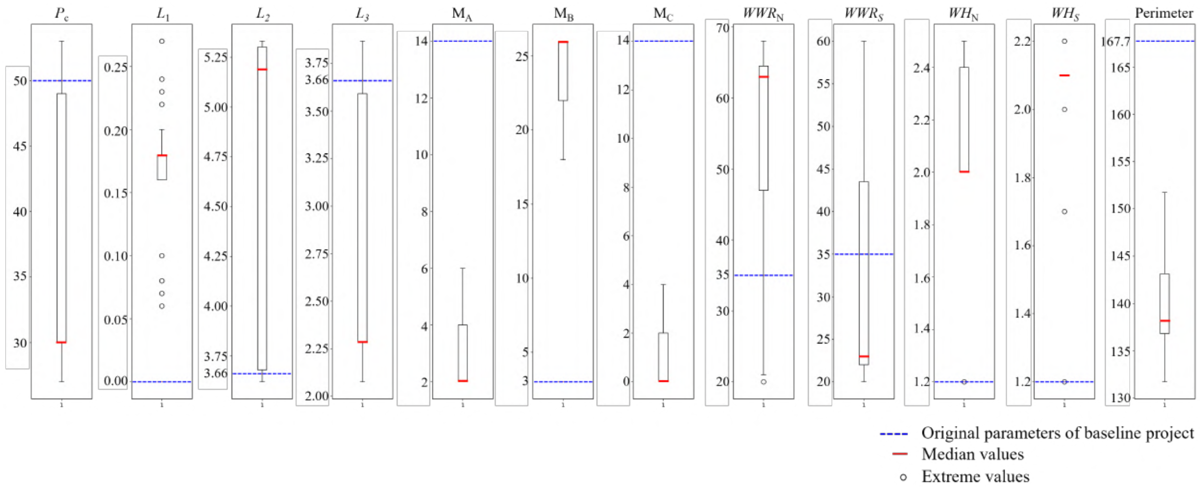

Figure 8. Comparison of 11 design parameters and the layout perimeter between 39 MiC Pareto optimal solutions and the baseline project.

Figure 8 compares the statistics of optimized design variables in the 39 MiC Pareto optima against the baseline design parameters. In the baseline solution, P_c is assigned as 50%, which means that the axis of the horizontal corridors is located in the middle of the core tube. As shown by the red bolded short line in the box plot, the median value of the optimized P_c was 30%, which means that the axis of the horizontal corridors is shifted towards south. The optimized values of L_2 are mainly distributed between 3.75m and 5.25m, which are slightly larger than the baseline parameters (3.66m). L_2 is utilized to modify the length of the sub-corridor on the north side, and a smaller P_c value would also mean an increase in L_2. The optimized values of L_3 are slightly smaller than the baseline parameters (3.66m), with the median of 2.26m. In contrast, the difference between the median value of optimized L_1 and the baseline solution is tiny, at 0.17m.

Meanwhile, the three types of modules are distributed in distinct ways. Figure 8 shows that the data spread of three types of modules is relatively concentrated. The number of M_B is significantly higher than the baseline scheme, with a median of 26. The total number for M_A is slightly lower than that of M_C, with median values of 2 and 0, respectively.

The optimized window design parameters vary considerably from the baseline parameters, especially for the WWR_N, and WWR_S. In the baseline scheme, the WWR_N and WWR_S were designed with an equal value of 35%, while the WH_N and WH_S were both in 1.2m.

However, the optimized WWR_N shows higher values, predominantly between 47% and 64%. The values for the optimized WWR_S, on the other hand, are mainly distributed between 21% and 40%. With regard to the height of the windows, the optimal solutions emphasize the almost same height of the windows on the north side (WH_N) and the south side (WH_S). The median value of the window's height on the north is 2.0m, while the value is 2.1m for the south side. Moreover, the optimized schemes' median perimeter value is roughly 137m, which is substantially less than the baseline project's perimeter value of 167.7m, indicating that the optimized schemes were more compact.

4.3 Sensitivity analysis

A sensitivity analysis was conducted to identify a cost-effective MOO setting from the aspects of daylighting simulation grid size and total population size. The grid size substantially influences the quantity of sensors utilized in daylight simulations, which subsequently affects the sDA computation outcomes and the simulation time frame. In the preliminary study, six grid sizes (i.e., 0.1 m, 0.2 m, 0.5m, 1m, 1.5m, and 2m) were selected for daylighting simulation of the baseline model, and the corresponding simulation times required for each case were documented, as illustrated in Figure 9. The computing time exhibited a substantial increase when the grid size was reduced to less than 0.5 m. E.g., a 0.2 m grid necessitated 135 seconds for computation, whereas a 0.1 m grid demanded 454 seconds. For the case in this paper, Figure 9 suggests that there was an 'elbow point' around time = 60s. Thus, a grid size of 0.5 m was selected to maintain a reasonable trade-off between computation time (i.e., 48 seconds per simulation on average) and accuracy.

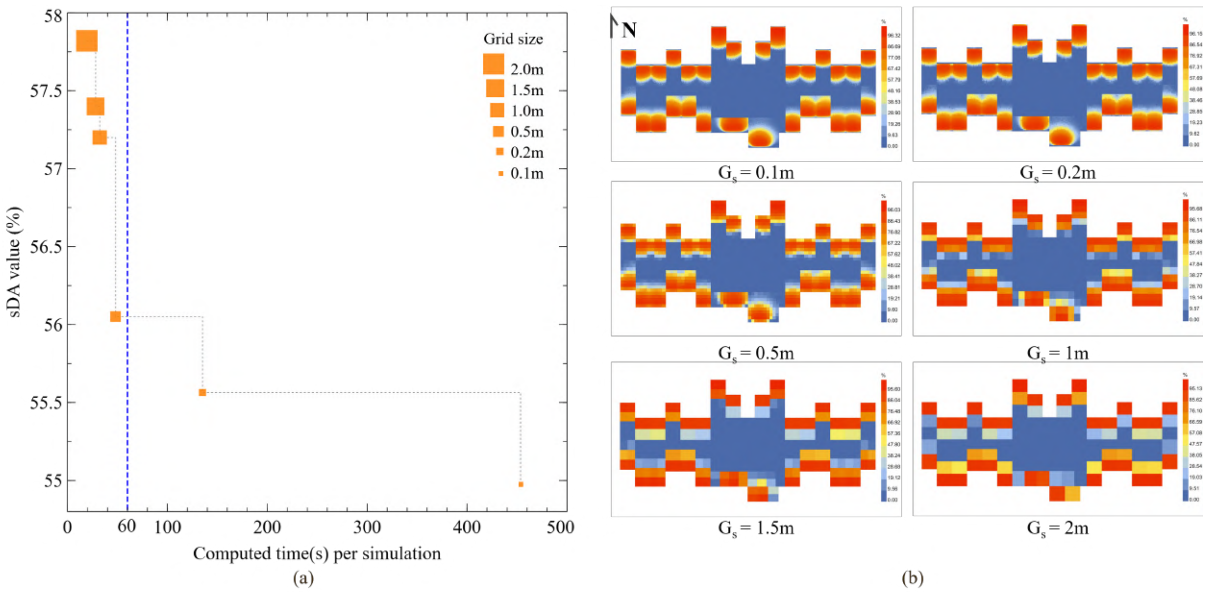

Figure 9. Sensitivity testing results of grid size for daylighting simulation. (a) The sDA values and time required for each simulation against grid size (dashed line indicates 60s); (b) Daylighting simulation results.

Figure 10 compares the number and location of the Pareto optimal solutions in three situations: total population size in 100 (10 chromosomes times by 10 generations), 625, and

2500. The experiments led to 14, 39, and 90 Pareto optima in 2.28 h, 15.56 h, and 72.48 h, respectively. In Figure 10 (a), there was only one Pareto optimum in the Pareto-Utopia shaded area when the population was 100. In contrast, the number of the most promising Pareto optima reached 16 after examining the population of 2,500, as shown in Figure 10 (c). In Figure 10 (c), the new Pareto optima in the shaded area progressed the five options in Figure 10 (b) to a limited extent, but it required a significant amount of time and effort for the decision-makers to compute and compare the final optimal solutions. Therefore, increasing the population size can generate slightly more promising solutions, at the costs of computer time for computation and experts' time for narrowing down the candidate MiC schemes for decision-makers.

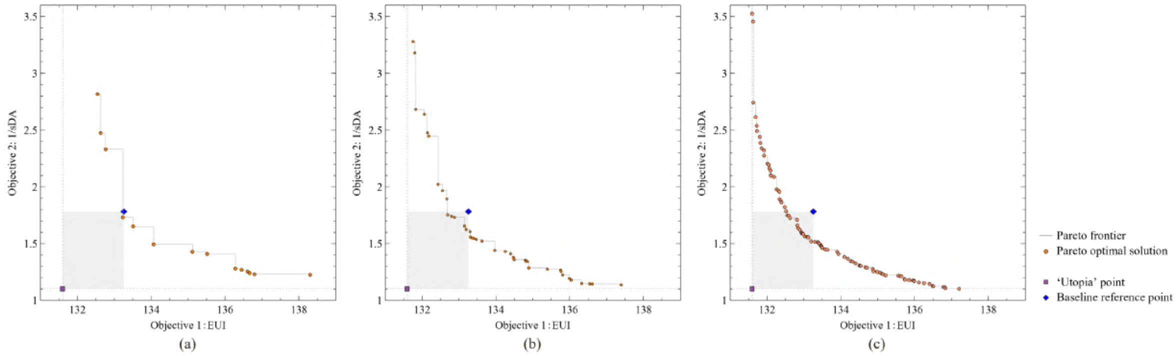

Figure 10. Scatter plot of Pareto optima against the population size of NSGA-II. (a) Population size as 100; (b) Population size as 625; (c) Population size as 2,500.

5 Discussion

The SSG-MMO method presented in this paper shows promising experimental results in improving ambient daylighting and reducing operational energy costs in the early design phase of MiC projects. The three-level comparative analysis provides an efficient and elaborate way of analyzing the information in the MiC Pareto optima. By subject to the target gross floor area, the decision-makers have the flexibility to compare multiple Pareto optimal solutions under a defined number of occupants. In terms of modular layout, the optimized MiC designs arrange more M_B than the baseline one and tends to be essentially flat at the northern boundary. According to Spearman's correlation analysis, the value of WWR_N, and WWR_S have a robust correlation with optimizing the energy efficiency and daylight performance in the Hong Kong region.

Therefore, the optimized parameters for MiC window and corridor design can also be summarized into valuable suggestions for energy-efficient design strategies. Specifically, the optimized window design parameters indicate that the window ratio should be distinguished for the north and south sides, while the values of WWR should be increased on the north side. Meanwhile, the optimized P_c suggests that the corridors' layout becomes more passive energy efficient as it is shifted southward. The optimization results for the window and corridor parameters are consistent with the geographical location and climatic conditions of Hong Kong. Therefore, for Hong Kong in a subtropical climate, the energy-efficient MiC designs (with a due north orientation) should increase the ratio of windows on the north side of the building and design the axis of the horizontal corridor towards the southern part of the core, as well as reduce the concavity of the northern boundary.

However, there are three groups of limitations in this paper. Firstly, there are limitations in the SSG-MOO formulation. This paper mainly conducts optimization from energy consumption and daylighting aspects, without other operational performance indicators for MiC design, such as target wind load, ventilation, personalized thermal comfort, and carbon emissions. Also, the envelope optimization in this paper concerns the size of the windows regardless of the influence of different materials and coating on energy efficiency. Therefore, the conclusive design tactics may be overridden by other design needs in practice. Secondly, this paper is limited in applying NSGA-II as the only algorithm. In the future, other MOO algorithms, such as CMA-ES and PSO, are also potential to solve the SSG-MOO problem for MiC. Lastly, the numerical computational results need further validation and comments by field experts.

6 Conclusion

Novel construction technologies are required with lifecycle passive designs to address energy crises and comfort concerns. This paper presents a symmetric skeleton grammar to handle the constrained MiC designs and MOO to cope with the exponential combinations of various modules for energy efficiency and daylight autonomy in the operational phase. A pilot MiC project was studied in Hong Kong to evaluate the proposed method. By optimizing 11 design variables regarding windows, corridors, and layouts of MiC modules, five optimized options were selected from 39 Pareto optima using the Pareto-Utopia shaded screening method. Meanwhile, the optimal design tactics can be summarized to passive MiC designs for energy efficiency and daylight autonomy: (i) the ratio of north-facing windows (WWR_{N}) should be increased, and (ii) the axis of the horizontal corridor should move southward, while maintaining flatness at the northern boundary.

The main contribution of this paper can be concluded in two aspects. From the MiC researchers' perspective, the method presents a symmetric skeleton grammar of MiC designs. Moreover, the proposed bi-objective formulation optimizes the parametric MiC designs in an energy-efficient and sufficient daylighting manner. From the industrial practitioners' perspective, the SSG-MOO with Pareto-Utopia-shaded screening method can efficiently assist designers in selecting the optimized solution(s) with multi-level evidence-based information. And valuable energy-efficient design strategies can be suggested for MiC designers in Hong Kong.

In the future, researchers can broaden the goals of MiC design optimization for wind load, thermal comfort, and carbon emissions, and taking into account the impact of different envelope materials on building performance. Furthermore, advanced MOO algorithms can be studied and applied to address the complex SSG-MOO problems. In addition, human experts can be included in the loop to verify and guide the Pareto optima selection for multi-level evidence-based decision making.

Acknowledgment

The study was supported by Hong Kong Research Grants Council (RGC) (Nos. 27200520, C7080-22GF, T22-504/21-R).

References

Abdelmageed, S. & Zayed, T. (2020). A study of literature in modular integrated construction - Critical review and future directions. *Journal of Cleaner Production, 277*, 124044. doi:10.1016/j.jclepro.2020.124044

Ascione, F., Bianco, N., Masi, R. F., Mauro, G. M. & Vanoli, G. P. (2017). Resilience of robust cost-optimal energy retrofit of buildings to global warming: A multi-stage, multi-objective approach. *Energy and Buildings, 153*, 150-167. doi:10.1016/j.enbuild.2017.08.004

ASHRAE. (2021). *Weather Data Viewer.* Retrieved 12 21, 2022, from https://www.ashrae.org/technical-resources/bookstore/weather-data-center#weather

Baños, R., Manzano-Agugliaro, F., Montoya, F., Gil, C., Alcayde, A. & Gómez, J. (2011). Optimization methods applied to renewable and sustainable energy: A review. *Renewable and Sustainable Energy Reviews, 15*(4), 1753-1766. doi:10.1016/j.rser.2010.12.008

Chantrelle, F. P., Lahmidi, H., Keilholz, W., Mankibi, M. E. & Michel, P. (2011). Development of a multicriteria tool for optimizing the renovation of buildings. *Applied Energy, 88*(4), 1386-1394. doi:10.1016/j.apenergy.2010.10.002

Ciardiello, A., Rosso, F., Dell'Olmo, J., Ciancio, V., Ferrero, M. & Salata, F. (2020). Multi-objective approach to the optimization of shape and envelope in building energy design. *Applied Energy, 280*, 115984. doi:10.1016/j.apenergy.2020.115984

Clarich, A., Russo, R. & Carriglio, M. (2011). Multi-objective optimization with modefrontier interfaces for ansa and metapost. *4th ANSA & μETA International Conference*, (pp. 1-16). Thessaloniki, Greece.

Clarke, J. & Hensen, J. (2015). Integrated building performance simulation: Progress, prospects and requirements. *Building and Environment, 91*, 294-306. doi:10.1016/j.buildenv.2015.04.002

Deb, K., Pratap, A., Agarwal, S. & Meyarivan, T. (2002). A fast and elitist multiobjective genetic algorithm: NSGA-II. *IEEE Transactions on Evolutionary Computation. 6(2)*, pp. 182 - 197. IEEE. doi:10.1109/4235.996017

Didier, G., Berangere, L. & Françoise, T. (2013). Multi-objective optimization of a building envelope for thermal performance using genetic algorithms and artificial neural network. *Energy and Buildings, 67*, 253-260. doi:10.1016/j.enbuild.2013.08.026

Duarte, J. P. (2005). Towards the mass customization of housing: The grammar Siza's houses at Malagueira. *Environment and planning B: Planning and Design, 32*(3), 347-380. doi:10.1068/b31124

Echenagucia, T. M., Capozzoli, A., Cascone, Y. & Sassone, M. (2015). The early design stage of a building envelope: Multi-objective search through heating, cooling and lighting energy performance analysis. *Applied Energy, 154*, 577–591. doi:10.1016/j.apenergy.2015.04.090

EMSD. (2022). *Hong Kong energy end-use data.* Retrieved 2 6, 2023, from https://www.emsd.gov.hk/filemanager/en/content_762/HKEEUD2022.pdf

Evins, R. (2013). A review of computational optimisation methods applied to sustainable building design. *Renewable and Sustainable Energy Reviews, 22*, 230-245. doi:10.1016/j.rser.2013.02.004

Fang, Y. & Cho, S. (2019). Design optimization of building geometry and fenestration for daylighting and energy performance. *Solar Energy, 191*, 7-18. doi:10.1016/j.solener.2019.08.039

Gan, V. J. (2022). BIM-based graph data model for automatic generative design of modular buildings. *Automation in Construction, 134*, 104062. doi:10.1016/j.autcon.2021.104062

Gan, V. J., Wong, H., Tse, K., Cheng, J. C., Lo, I. M. & Chan, C. (2019). Simulation-based evolutionary optimization for energy-efficient layout plan design of high-rise residential buildings. *Journal of Cleaner Production, 231*, 1375-1388. doi:10.1016/j.jclepro.2019.05.324

Gülen, Ç. (1996). A shape grammar: The language of traditional Turkish houses. *Environment and Planning B: Planning and Design*, *23*(4), 443-464. doi:10.1068/b230443

Haakonsen, S. M., Rønnquist, A. & Labonnote, N. (2023). Fifty years of shape grammars: A systematic mapping of its application in engineering and architecture. *International Journal of Architectural Computing*, *21*(1), 5-22. doi:10.1177/14780771221089882

Habash, R. (2022). Building as an energy system. In *Sustainability and Health in Intelligent Buildings* (pp. 59-94). Woodhead Publishing. doi:10.1016/B978-0-323-98826-1.00003-X

Hajela, P. & Lin, C. Y. (1992). Genetic search strategies in multicriterion optimal design. *Structural optimization*, *4*, 99–107. doi:10.1007/BF01759923

Hamdy, M., Nguyen, A.-T. & Hensen, J. L. (2016). A performance comparison of multi-objective optimization algorithms for solving nearly-zero-energy-building design problems. *Energy and Buildings, 121*, 57-71. doi:10.1016/j.enbuild.2016.03.035

Heschong, L., Wymelenberg, K. V., Andersen, M., Digert, N., Fernandes, L., Keller, A., Loveland, J., McKay, H., Mistrick, R., Mosher, B., Reinhart, C., Rogers, Z. & Tanteri, M. (2012). Approved Method: IES Spatial Daylight Autonomy (sDA) and Annual Sunlight Exposure (ASE). In *IES* (pp. LM-83-12). New York: Illuminating Engineering Society of North America. Retrieved 2 15, 2023, from https://www.usgbc.org/resources/ies-lighting-measurements-lm-83-12-approved-method-ies-spatial-daylight-autonomy-sda-and-a

HKHA. (2020, October 30). *Standard Block Typical Floor Plans.* Hong Kong: Hong Kong Housing Authority. Retrieved 12 21, 2022, from https://www.housingauthority.gov.hk/en/global-elements/estate-locator/standard-block-typical-floor-plans/

HKHA. (2022). *Publication Archive: 2021/22 Annual Report.* Hong Kong: Hong Kong Housing Authority. Retrieved 12 21, 2022, from https://www.housingauthority.gov.hk/en/about-us/publications-and-statistics/publication-archive/index.html

HKSAR. (2021). *Information paper provided by the Administration concerning the annual progress report on implementation of Hostel Development Fund.* Hong Kong: Legislative Council of the Hong Kong Special Administrative Region. Retrieved 12 21, 2022, from https://www.legco.gov.hk/yr20-21/english/panels/ed/papers/edcb4-1645-1-e.pdf

Koning, H. & Eizenberg, J. (1981). The language of the prairie: Frank Lloyd Wright's prairie houses. *Environment and Planning B: Urban Analytics and City Science, 8*(3), 295-323. doi:10.1068/b080295

Konis, K., Gamas, A. & Kensek, K. (2016). Passive performance and building form: An optimization framework for early-stage design support. *Solar Energy*, *125*, 161-179. doi:10.1016/j.solener.2015.12.020

Li, M., Xue, F. & Yeh, A. G. (2023). Bi-objective analytics of 3D visual-physical nature exposures in high-rise high-density cities for landscape and urban planning. *Landscape and Urban Planning*, *233*, 104714. doi:10.1016/j.landurbplan.2023.104714

Li, X., Lu, W., Xue, F. & Wu, L. (2022). Blockchain-Enabled IoT-BIM Platform for Supply Chain Management in Modular Construction. *Journal of Construction Engineering and Management*, *148*(2), 04021195. doi:10.1061/(ASCE)CO.1943-7862.0002229

Li, X., Wu, C., Xue, F., Yang, Z., Lou, J. & Lu, W. (2022). Ontology-based mapping approach for automatic work packaging in modular construction. *Automation in Construction*, *134*, 104083. doi:10.1016/j.autcon.2021.104083

Liu, S., Kwok, Y. T., Lau, K. K.-L., Ouyang, W. & Ng, E. (2020). Effectiveness of passive design strategies in responding to future climate change for residential buildings in hot and humid Hong Kong. *Energy and Buildings*, *228*, 110469. doi:10.1016/j.enbuild.2020.110469

Ljung, L. & Singh, R. (2012). Version 8 of the Matlab System Identification Toolbox. *IFAC Proceedings Volumes*, *45*(16), 1826-1831. doi:10.3182/20120711-3-BE-2027.00061

Makki, M., Farzaneh, A. & Navarro, D. (2015). The Evolutionary Adaptation of Urban Tissues through Computational Analysis. *Real time-Proceedings of the 33rd eCAADe Conference. 2*, pp. 563-571. Vienna: Vienna University of Technology. doi:10.52842/conf.ecaade.2015.2.563

Makki, M., Showkatbakhsh, M. & Song, Y. (2018). *Wallacei - An Analytic and Evolutionary Engine for Grasshopper 3D.* Retrieved 12 21, 2022, from https://www.wallacei.com/

McNeel, R. (2023). *Grasshopper®(Version 1.0.0007): algorithmic modeling for Rhino*. Retrieved 7 7, 2023, from https://www.grasshopper3d.com/

Nguyen, A.-T., Reiter, S. & Rigo, P. (2014). A review on simulation-based optimization methods applied to building performance analysis. *Applied Energy*, *113*, 1043-1058. doi:10.1016/j.apenergy.2013.08.061

Ning, G. & Peiman, A. B. (2018). Shape Grammars: A Key Generative Design Algorithm. In *Handbook of the Mathematics of the Arts and Sciences* (pp. 1385-1405). Springer International Publishing.

Pan, W. & Hon, C. K. (2020). Briefing: Modular integrated construction for high-rise buildings. *Proceedings of the Institution of Civil Engineers-Municipal Engineer. 173*, pp. 64-68. Thomas Telford Ltd. doi:10.1680/jmuen.18.00028

Paulino, D. M., Ligler, H. & Napolitano, R. (2023). A Grammar-Based Approach for Generating Spatial Layout Solutions for the Adaptive Reuse of Sobrado Buildings. *Buildings*, *13*(3), 722. doi:10.3390/buildings13030722

Pilechiha, P., Mahdavinejad, M., Rahimian, F. P., Carnemolla, P. & Seyedzadeh, S. (2020). Multi-objective optimisation framework for designing office windows: quality of view, daylight and energy efficiency. *Applied Energy*, *261*, 114356. doi:10.1016/j.apenergy.2019.114356

Qin, H. & Pan, W. (2020). Energy use of subtropical high-rise public residential buildings and impacts of energy saving measures. *Journal of Cleaner Production*, *254*, 120041. doi:10.1016/j.jclepro.2020.120041

Roudsari, M. S. & Pak, M. (2013). Ladybug: A parametric environmental plugin for grasshopper to help designers create an environmentally-conscious design. *Proceedings of the 13th international IBPSA conference* (pp. 3128-3135). Lyon, France: Building Simulation Conference Proceedings. doi:10.26868/25222708.2013.2499

Ruiz-Montiel, M., Boned, J., Gavilanes, J., Jiménez, E., Mandow, L. & Pérez-de-la-Cruz, J.-L. (2013). Design with shape grammars and reinforcement learning. *Advanced Engineering Informatics*, *27*(2), 230-245. doi:10.1016/j.aei.2012.12.004

Sadineni, S. B., Madala, S. & Boehm, R. F. (2011). Passive building energy savings: A review of building envelope components. *Renewable and Sustainable Energy Reviews, 15*(8), 3617-3631. doi:10.1016/j.rser.2011.07.014

Showkatbakhsh, M. & Makki, M. (2022). Multi-Objective Optimisation of Urban Form: A Framework for Selecting the Optimal Solution. *Buildings*, *12*(9), 1473. doi:10.3390/buildings12091473

Stevanović, S. (2013). Optimization of passive solar design strategies: A review. *Renewable and Sustainable Energy Reviews, 25*, 177-196. doi:10.1016/j.rser.2013.04.028

Stiny, G. & Gips, J. (1972). Shape Grammars and the Generative Specification of Painting and Sculpture. *IFIP Congress* (pp. 1460–1465). Amsterdam: Information Processing 71. Retrieved from https://citeseerx.ist.psu.edu/document?repid=rep1&type=pdf&doi=6dc9c55dade136193780a3ce0f5269036c5127cf

Stiny, G. & Mitchell, W. J. (1978). The palladian grammar. *Environment and planning B: Planning and design, 5*(1), 5–18. doi:10.1068/b050005

Tian, Z., Zhang, X., Jin, X., Zhou, X., Si, B. & Shi, X. (2018). Towards adoption of building energy simulation and optimization for passive building design: A survey and a review. *Energy and Buildings, 158*, 1306-1316. doi:10.1016/j.enbuild.2017.11.022

UNEP. (2022). *Global Status Report for Buildings and Construction: Towards a Zero-emission, Efficient and Resilient Buildings and Construction Sector.* Nairobi: United Nations Environment Programme (UNEP). Retrieved 3 9, 2023, from https://www.unep.org/resources/publication/2022-global-status-report-buildings-and-construction

USGBC. (2022). *Daylight | Indoor Environmental Quality*. U.S. Green Building Council. Retrieved 12 21, 2022, from https://www.usgbc.org/credits/new-construction-schools-new-construction-retail-new-construction-data-centers-new-9

Wang, M., Wang, C. C., Sepasgozar, S. & Zlatanova, S. (2020). A Systematic Review of Digital Technology Adoption in Off-Site Construction: Current Status and Future Direction towards Industry 4.0. *Buildings*, *10*(11), 204. doi:10.3390/buildings10110204

Zhang, J., Liu, N. & Wang, S. (2021). Generative design and performance optimization of residential buildings based on parametric algorithm. *Energy and Buildings, 244*, 111033. doi:10.1016/j.enbuild.2021.111033

Zheng, L., Lu, W., Wu, L. & Zhou, Q. (2023). A review of integration between BIM and CFD for building outdoor environment simulation. *Building and Environment, 228*, 109862. doi:10.1016/j.buildenv.2022.109862